

SCIENTIA MARINA 84(1)
March 2020, 71-82, Barcelona (Spain)
ISSN-L: 0214-8358
<https://doi.org/10.3989/scimar.04972.17B>

Decapod crustacean larval community structure of the submarine canyon off Blanes (NW Mediterranean Sea)

Marta Carreton¹, Joan B. Company¹, Alexandra Boné¹, Guiomar Rotllant¹, Guillermo Guerao², Nixon Bahamon^{1,3}, María Inés Roldán⁴, Antonina dos Santos^{5,6}

¹ Institut de Ciències del Mar, CSIC. Passeig Marítim de la Barceloneta 37-49, 08003 Barcelona, Spain.
(MC) (Corresponding author) E-mail: mcarreton@icm.csic.es. ORCID iD: <https://orcid.org/0000-0002-9490-1453>
(JBC) E-mail: batista@icm.csic.es. ORCID iD: <https://orcid.org/0000-0002-5878-7155>
(AB) E-mail: alexandrabonefernandez@gmail.com. ORCID iD: <https://orcid.org/0000-0002-7551-8045>
(GR) E-mail: guio@icm.csic.es. ORCID iD: <https://orcid.org/0000-0002-6692-9678>

² Institut de Recerca i Tecnologia Agroalimentàries (IRTA), Ctra. de Poble Nou 5, 43540 Sant Carles de la Ràpita, Tarragona, Spain.
(GG) E-mail: gguerao@gmail.com. ORCID iD: <https://orcid.org/0000-0001-9738-7923>

³ Centre d'Estudis Avançats de Blanes (CEAB-CSIC). C/ d'accés a la Cala St. Francesc, 14, 17300 Blanes, Girona, Spain.
(NB) E-mail: n.bahamon@csic.es. ORCID iD: <https://orcid.org/0000-0002-5802-7367>

⁴ Laboratori d'Ictiologia Genètica, Universitat de Girona, Maria Aurelia Capmany 40, 17003 Girona, Spain.
(MIR) E-mail: marina.roldan@udg.edu. ORCID iD: <https://orcid.org/0000-0003-3936-3522>

⁵ Instituto Português do Mar e da Atmosfera (IPMA), Av. Alfredo Magalhães Ramalho, 6, 1495-165 Lisboa, Portugal.

⁶ CIIMAR – Interdisciplinary Centre of Marine and Environmental Research, Porto, Portugal.
(ADS) E-mail: antonina@ipma.pt. ORCID iD: <https://orcid.org/0000-0002-2238-9315>

Summary: Decapod crustacean fisheries play a crucial role on the northwestern Mediterranean coast due to their high commercial value. Although knowledge of larval ecology and recruitment dynamics of these species is essential to establish a sustainable fisheries management, they are still poorly known. In this paper, we describe the composition, abundance and distribution of decapod crustacean larvae in the submarine canyon off Blanes (northwestern Mediterranean Sea) during summer thermal stratification conditions. Samples were collected in September 2011 with a multi-net system and a 60-cm bongo net at 22 stations with bottom depths of between 100 and 1800 m. A total of 635 larvae from 60 genera were identified. The most relevant taxa were *Aristeus antennatus* (7.93 individuals/1000 m³), the family Sergestidae (7.24) and *Alpheus glaber* (6.78). These three taxa were dominant (>20% of total decapod larvae) at more than half of the stations. Decapod larval communities were found to be richer and more diverse at the canyon head, a finding which could be explained by the higher retention rates when compared with the upstream and downstream walls and the canyon axis.

Keywords: decapod larvae; submarine canyons; Mediterranean Sea; zooplankton; *Aristeus antennatus*.

Estructura de la comunidad larvaria de crustáceos decápodos del cañón submarino de Blanes (Mediterráneo noroccidental)

Resumen: Las pesquerías de crustáceos decápodos juegan un papel crucial en la costa del Mediterráneo noroccidental debido a su alto valor comercial. Aunque la información sobre la ecología larvaria y las dinámicas de reclutamiento de estas especies es esencial para establecer una gestión sostenible de estas pesquerías, estos aspectos son aún poco conocidos. En este estudio, se describe la composición, abundancia y distribución de las larvas de crustáceos decápodos en el cañón submarino de Blanes (Mediterráneo noroccidental) durante las condiciones de estratificación térmica estival. Las muestras fueron tomadas en septiembre de 2011 con un sistema multi-red y una red bongo de 60 cm de diámetro en 22 estaciones con fondos de entre 100 y 1800 m de profundidad. Un total de 635 larvas de 60 géneros fueron identificadas. Los taxones más relevantes fueron *Aristeus antennatus* (7.93 individuos/1000 m³), la familia Sergestidae (7.24) y *Alpheus glaber* (6.78). Estos tres taxones fueron dominantes (>20% del total de larvas de decápodos) en más de la mitad de las estaciones. Se encontró que las comunidades larvarias de decápodos son más ricas y diversas en la cabecera del cañón, lo cual podría explicarse por los altos índices de retención que presenta esta zona en comparación con las paredes del cañón y su eje.

Palabras clave: larvas de decápodos; cañones submarinos; Mediterráneo; zooplankton; *Aristeus antennatus*.

Citation/Como citar este artículo: Carreton M., Company J.B., Boné A., Rotllant G., Guerao G., Bahamon N., Roldán M.I., dos Santos A. 2020. Decapod crustacean larval community structure of the submarine canyon off Blanes (NW Mediterranean Sea). *Sci. Mar.* 84(1): 71-82. <https://doi.org/10.3989/scimar.04972.17B>

Editor: J.A. Cuesta.

Received: July 1, 2019. **Accepted:** December 3, 2019. **Published:** January 29, 2020.

Copyright: © 2020 CSIC. This is an open-access article distributed under the terms of the Creative Commons Attribution 4.0 International (CC BY 4.0) License.

INTRODUCTION

Submarine canyons are known to be hotspots for biodiversity (Gili et al. 2000, De Leo et al. 2010). Their geomorphology shapes the sediment transport patterns on the continental margin, enhancing productivity as they play the role of particulate and organic matter traps (Granata et al. 1999). Previous studies on such structures have shown that particles from shallow coastal adjacent areas can be transported into the greater depths of the canyon axis, where they sink to the bottom due to reduced horizontal advection and higher residence time (Ahumada-Sempoal et al. 2015). This phenomenon fertilizes the sea bottom and benefits benthic communities.

The western Mediterranean continental margin is cut by several submarine canyons, some of which have been thoroughly studied from a fisheries management perspective. These canyons are important fishing grounds for many fish and crustacean species of both ecological and commercial interest, which also use these areas as spawning, nursery or recruitment zones (Sardà et al. 2009, Fernandez-Arcaya et al. 2013). Among these species, decapod crustaceans are the most valuable group for the local fisheries industry, ranking the highest in selling prices. For instance, the deep-sea blue and red shrimp *Aristeus antennatus*, targeted by the bottom-trawling fleet in the submarine canyon areas, can account for up to 50% of the fishermen's associations annual revenue and is subject to a local management plan in the area of Palamós, north of Blanes (BOE 2018).

Although most decapod crustacean species in the northwestern Mediterranean Sea have been widely studied in their adult form (Maynou et al. 1996, Company and Sardà 2000, Company et al. 2003), little is still known about their larval abundance and distribution, and even less in the case of deep-sea species due to the difficulty of sampling in offshore locations. This information is essential to assess the species dispersal and connectivity patterns. In the case of *A. antennatus*, only five larval stages have been described using morphological methods and confirmed by analysing molecular markers: the first protozoa (PZ I), subsequent to the hatched naupliar phase, protozoa II (PZ II), protozoa III (PZ III), mysis I (M I) and mysis II (M II) (Heldt 1955, Torres et al. 2014a, Carreton et al. 2019). As illustrated in a recent study, the PZ I of *A. antennatus* is morphologically very similar to that of *Gennadas elegans*, a small mesopelagic shrimp of no commercial interest, and the correct identification of this stage calls for a combination of morphological and molecular methods (Carreton et al. 2019, Carreton et al. unpubl data). First, these PZ I are distinguished morphologically from the rest of Dendrobranchiata PZ I by their smooth carapace, third maxilliped present, and antennule and antenna of similar length (dos Santos and Lindley 2001). They are then analysed through barcoding to differentiate whether they belong to *A. antennatus* or *G. elegans*. Although further stages can be clearly identified using only morphological characters, this difficulty

with the PZI larvae is a drawback in decapod larval ecology studies in the northwestern Mediterranean Sea, where both species are an important part of the plankton community. In this area, previous studies on zooplankton have mainly focused on brachyuran crab larvae (Abelló 1989, Abelló and Guerao 1999) and others have given a broader view of the decapod larval community (Fusté 1987). It was only recently that a study tackled the larval distribution of decapod crustaceans in commercial fishing grounds, showing an occurrence of 25% of *A. antennatus* larvae in the Balearic Sea with an average abundance of 0.1 ind./1000 m³ (Torres et al. 2013). However, to our knowledge no studies have been reported in submarine canyon areas of the Mediterranean, despite their critical role in the reproduction of these species (Sardà et al. 2009). The recurrent meanders and eddies that affect submarine canyons produce a highly fluctuating hydrodynamic circulation pattern and transport (Ahumada-Sempoal et al. 2013). Settlement of decapod larvae has also been proved to respond to hydrodynamic conditions (Criales et al. 2013, 2015), so it is particularly interesting to acquire knowledge of larval distribution in these areas.

Blanes submarine canyon incises the continental margin of the northwestern Mediterranean Sea, from 41°N to 41.8°N and from 2.7°E to 3.2°E, off Blanes port. It has a north-south orientation and its width increases with depth until it reaches a maximum of 23 km at 2600 m depth (Canals et al. 2013). The continental shelf in this area of the eastern Iberian Peninsula is relatively narrow, with the upper canyon located only 4 km from the coastline. It is a deep and narrow canyon with a smooth eastern (upstream) wall and a sharp and abrupt western (downstream) wall. Water circulation in the area is generally cyclonic along the continental slope, as a result of the combination of the Atlantic Water arriving through the Gibraltar Strait and the Northern Current coming from north to south from the Gulf of Lions (Flexas et al. 2008). The authors suggest that the speed of the Northern Current starts to increase by the end of summer, entering the canyon, and reaches its maximum in the winter months, when the mixed layer becomes thicker. The interaction of the predominant SW flow with the bottom topography of the canyons may produce transient local mesoscale eddies and anticyclonic gyres over the continental shelf, thus causing "inversions" of the circulation pattern in the area northeastward (Rubio et al. 2005, Ahumada-Sempoal et al. 2013). Given the particularities of the geomorphology in the submarine canyon, hydrodynamics is likely to influence the larval distribution and abundance of particles and pelagic life forms such as eggs and larvae by modifying the retention rates and transport dynamics (Ahumada-Sempoal et al. 2013). The anticyclonic gyres produced over the canyon head may force them to aggregate over the shelf break around 150 m depth (Ahumada-Sempoal et al. 2015).

The present study aimed to assess the composition, distribution and abundance of the decapod larval community in Blanes submarine canyon under summer thermal stratification conditions. In particular, we ex-

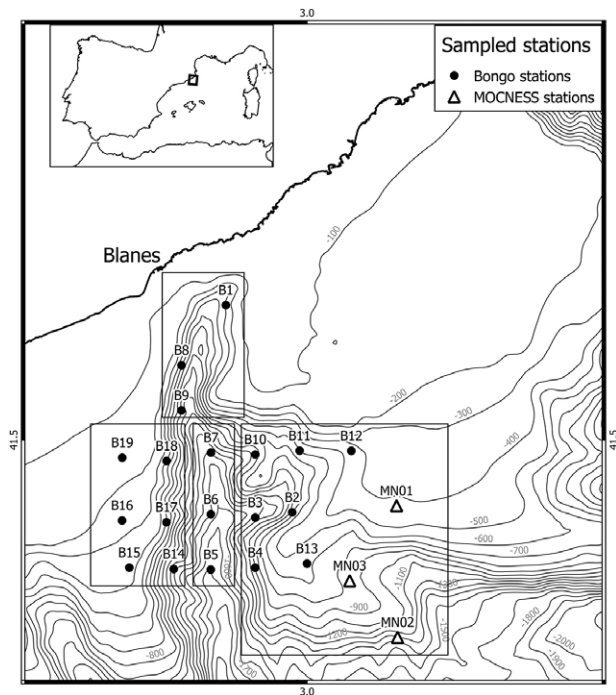


Fig. 1. – Sampling locations in the Blanes submarine canyon area. Canyon zones are indicated by rectangles: canyon head (top), downstream wall (bottom left), canyon axis (bottom centre), and upstream wall (bottom right).

pected to find the larvae of the deep-sea blue and red shrimp *Aristeus antennatus*, as the area is one of its main nursery grounds in the northwestern Mediterranean Sea. The linkage of the community structure with hydrological conditions is discussed.

MATERIALS AND METHODS

Zooplankton sampling

Sampling was conducted in the framework of the project “Observation, Analysis and Modelling of the Mediterranean Sea” (OAMMS, CTM2008-03983). The cruise was carried out in Blanes submarine canyon (NW Mediterranean) on board the Spanish R/V *García del Cid*, from 26 to 29 September 2011. Twenty-two stations were sampled within the study area over bottoms of 123 to 1716 m depth. We used a 60-cm bongo at 19 of the stations and a multiple opening/closing net and environmental sensing system (MOCNESS, Wiebe et al. 1976) at the remaining three (Fig. 1). Three stations (B1, B8 and B9) were sampled at the canyon head, ten were sampled along the canyon’s upstream wall (B2, B3, B4, B10, B11, B12, B13, MN1, MN2 and MN3), six were sampled along its downstream wall (B14 to B19), and three were sampled along the canyon axis (B5, B6 and B7). Sampling depth and gear were established according to the station bottom depth (Tables 1 and 2).

The bongo was used to collect integrated samples from a maximum depth of 300 m to the surface in oblique tow at a speed of 2 kn. The two nets of the bongo carried different mesh sizes, 300 μ m and 500 μ m, to target different larval stages. These two nets

Table 1. – Information on the stations sampled with the Bongo net.

Station	Lat. (N)	Long. (E)	Sampling depth (m)	Bottom depth (m)
B1	41.637	2.891	100	123
B2	41.427	2.980	300	840
B3	41.422	2.932	300	1242
B4	41.371	2.932	300	940
B5	41.369	2.872	300	1716
B6	41.425	2.869	300	1360
B7	41.488	2.870	300	1202
B8	41.576	2.826	200	394
B9	41.530	2.835	300	775
B10	41.486	2.932	300	958
B11	41.490	2.992	300	566
B12	41.489	3.055	300	445
B13	41.375	3.000	300	650
B14	41.369	2.823	300	1206
B15	41.371	2.764	200	366
B16	41.418	2.748	200	268
B17	41.417	2.811	300	500
B18	41.479	2.812	300	438
B19	41.482	2.751	120	164

will hereinafter be referred to as B300 and B500, respectively. Both nets were equipped with a flow meter for filtered water volume calculations. The MOCNESS was used to collect stratified samples up to 900 m depth, carrying nine nets in a 1 m² mouth, mesh size being 300 μ m for N1 and N9 and 500 μ m for N2 to N8. An integrated sample (N1) was taken from the surface to the maximum programmed sampling depth. Nets N2 to N9 were closed remotely from the vessel so that each stratum covered between 50 and 100 m depth of the water column (Table 2).

Physical data gathering

Information on the water column was gathered with a Teledyne RD Instruments Acoustic Doppler Current Profiler at 76.8 kHz. Reanalysis products from Copernicus Marine Environment Monitoring System were plotted in QGIS to provide a representative sea surface current field. Meteorological and oceanographic data collected from the oceanographic buoy moored at Blanes canyon head and led by the Operational Observatory of the Catalan Sea (OOCs, Bahamon et al. 2011) of CEAB-CSIC were obtained from the OOCs database.

Larval identification

Morphological identification

All plankton samples were fixed in situ in 5% formaldehyde buffered with sodium tetraborate. The samples were then sorted in the laboratory using a Leica M205 C stereomicroscope, and the decapod crustacean larvae were counted, staged and identified to the lowest possible taxonomical level. We focused on zoal stages only (protozoa and mysis in the case of the Dendrobranchiata), not accounting for the decapodid stages in the samples. For the identification of the larvae, we followed identification keys by dos Santos and Lindley (2001) and dos Santos and González-Gordillo (2004) and the checklist by González-Gordillo et al. (2001).

Table 2. – Information on the stations sampled with the MOCNESS sampler.

Station	Net	Mesh size (µm)	Initial lat. (N)	Final lat. (N)	Initial long. (E)	Final long. (E)	Net opening depth (m)	Net closing depth (m)	Bottom depth (m)
MN01	N8	500	41.436	41.434	3.121	3.121	50	0	381
	N7	500	41.438	41.436	3.121	3.121	100	50	393
	N6	500	41.440	41.438	3.121	3.121	150	100	400
	N5	500	41.442	41.440	3.121	3.121	200	150	419
	N4	500	41.444	41.442	3.121	3.121	250	200	445
	N3	500	41.447	41.444	3.121	3.121	300	250	459
	N2	500	41.451	41.447	3.121	3.121	350	300	436
	N1	300	41.487	41.451	3.123	3.121	350	0	436
MN02	N9	300	41.300	41.296	3.122	3.122	100	0	1004
	N8	500	41.304	41.300	3.123	3.122	200	100	968
	N7	500	41.311	41.304	3.124	3.123	300	200	948
	N6	500	41.317	41.311	3.124	3.124	400	300	965
	N5	500	41.323	41.317	3.124	3.124	500	400	1000
	N4	500	41.328	41.323	3.125	3.124	600	500	1045
	N3	500	41.335	41.328	3.124	3.125	800	600	1135
	N2	500	41.338	41.335	3.124	3.124	900	800	1224
	N1	300	41.387	41.338	3.120	3.124	900	0	1321
MN03	N9	300	41.358	41.355	3.058	3.058	50	0	796
	N8	500	41.361	41.358	3.058	3.058	100	50	795
	N7	500	41.366	41.361	3.058	3.058	200	100	798
	N6	500	41.372	41.366	3.058	3.058	300	200	804
	N5	500	41.376	41.372	3.058	3.058	400	300	833
	N4	500	41.380	41.376	3.058	3.058	500	400	855
	N3	500	41.382	41.380	3.058	3.058	600	500	861
	N2	500	41.372	41.382	3.057	3.058	700	600	848
	N1	300	41.423	41.372	3.057	3.057	700	0	826

Molecular identification

For the larval stages that are not clearly distinguished using the available keys and descriptions (dos Santos and Lindley 2001, Heldt 1955, Gurney 1924), that is, the first protozoal stage of *Gennadas* spp. and *Aristeus antennatus*, a molecular analysis was performed in AllGenetics facilities (A Coruña, Spain) to determine the identity of the larvae. The small size of the larvae and their preservation in buffered formaldehyde called for a special approach in which a pool of larvae had to be analysed together to ensure a sufficient DNA concentration. From a total of 52 protozoa I larvae of the type *Gennadas/Aristeus* identified, we randomly selected 35 individuals from all stations where they were present (B1, B5, B6, B7, B8, B9, B10, B14, B15, B16, B17, B18 and B19, see Fig. 1) and extracted DNA from the pool. DNA isolation was carried out following a protocol for formalin-fixed material (Campos and Gilibert 2012). Briefly, the formaldehyde-driven protein-DNA cross-links were reversed by treatment in a heated alkaline buffer (120°C for 25 min in a 0.1 M NaOH, 1% SDS solution, pH=12). The hot alkali treatment was followed by a phenol-chloroform extraction. A negative control that contained no sample was processed along with the sample to check for contamination during DNA isolation.

For library preparation, a short 172-base pair fragment of the cytochrome oxidase I (COI) region was amplified using the primers CrustDF1 (5' GGT CWA CAA AYC ATA AAG AYA TTG G 3', Steinke et al. 2016) and CrustDR_int (designed by AllGenetics), to which the Illumina sequencing primer sequences were attached at their 5' ends. PCRs were carried out in a final volume of 25 µL containing 2.5 µL of template DNA, 0.5 µM of the primers, 12.5 µL of Supreme NZYTaq 2x

Green Master Mix (NZYTech) and ultrapure water up to 25 µL. The reaction mixture was incubated as follows: an initial denaturation at 95°C for 5 min, followed by 25 cycles of 95°C for 30 s, 50°C for 30 s, 72°C for 30 s and a final extension step at 72°C for 10 minutes. Two negative controls that contained no DNA were included to check for contamination during library preparation. The libraries were then purified and sequenced in a fraction of a MiSeq PE300 run (Illumina).

The raw data were demultiplexed, and the forward and reverse reads performed with FLASH (Magoc and Salzberg 2011). We used CUTADAPT (Martin 2011) and Qiime (Caporaso et al. 2010) to preprocess and quality-filter the data, keeping only sequences with a minimum Phred quality score of 20. The sequences were then dereplicated, clustered at a similarity threshold of 100% and sorted. The impact of point mutations and chimeras generated during PCR and sequencing was reduced by applying filters in the bioinformatic pipeline. The sequences were then assigned to operational taxonomic units (OTUs).

For taxonomic assignment, we created a local reference database by combining the COI sequence data available for the order Decapoda in the DDBJ/ENA/GenBank (<http://www.insdc.org>) and BOLD (<http://www.boldsystems.org>) databases. The reference database was length-filtered to exclude sequences shorter than 100 base pairs, and identical sequences were collapsed to a single entry. The taxonomic assignment of the OTU table was performed by querying the clustered centroids against the COI reference database with a 90% similarity threshold. Finally, the OTU table was quality-filtered to keep only the OTUs that matched any reference sequence in the reference database. At the end of the filtering process, the 314320 paired-end raw sequences produced a table with 147323 filtered

sequences. Illumina paired-end raw data are available at the Sequence Read Archive (Leinonen et al. 2010) operated by the National Center for Biotechnology Information under accession number PRJNA539861.

Data analysis

The number of larvae collected at each station was standardised to number of individuals per 1000 m³. These density data were log transformed (log(x+1)) to comply with statistical restrictions. The data were processed using R (R Development Core Team 2018) and QGIS (QGIS Development Team 2019). In order to evaluate the specificity of the two different mesh sizes of B300 and B500 for early (zoeas I to IV) and late (zoeas V onward) larval stages, respectively, the

average larval stage was calculated for each net and a one-way ANOVA was performed.

A non-metric multidimensional scaling (NMDS) representation of the data was produced with R. We calculated the Shannon-Wiener diversity index, species richness and the Pielou evenness index for each station, and a multivariate permutational analysis of variance using the Bray-Curtis distance matrix of the communities was carried out using the ‘vegan’ package (Oksanen et al. 2017) in R. Taxa identified up to taxonomic levels higher than genus were used in the spatial representation of the data but not accounted for in the diversity index calculations. Finally, an analysis of similarity was performed to test for community differences between canyon zones and a similarity percentage analysis (SIMPER) was used to determine

Table 3. – Total number (N), average density of individuals per 1000 m³ with standard deviation and frequency (F) of decapod larvae caught with bongo net.

Taxon	N	B300 Average density (ind./1000 m ³)	F (%)	N	B500 Average density (ind./1000 m ³)	F (%)
Suborder Dendrobranchiata						
<i>Aristeus antennatus</i>	52	8.00 ± 8.71	68.42	2	0.27 ± 1.17	5.26
<i>Sicyonia carinata</i>	2	0.33 ± 1.42	5.26	2	0.36 ± 1.59	5.26
<i>Solenocera membranacea</i>	9	1.17 ± 2.35	21.05	4	0.52 ± 1.37	15.79
<i>Eusergestes arcticus</i>	0	0.00	0.00	8	1.29 ± 4.47	15.79
<i>Sergestes atlanticus</i>	8	1.30 ± 5.69	5.26	0	0.00	0.00
Sergestidae	51	7.38 ± 8.66	73.68	14	1.99 ± 2.54	42.11
Suborder Pleocyemata						
<i>Pasiphaea</i> spp.	2	0.24 ± 1.05	5.26	0	0.00	0.00
<i>Acanthephyra</i> spp.	0	0.00	0.00	1	0.27 ± 1.18	5.26
<i>Alpheus glaber</i>	53	6.84 ± 7.49	78.95	41	4.74 ± 5.33	84.21
<i>Hippolyte</i> spp.	0	0.00	0.00	1	0.33 ± 1.44	5.26
<i>Eualus</i> spp.	1	0.12 ± 0.53	5.26	1	0.10 ± 0.45	5.26
<i>Lysmata</i> spp.	9	1.34 ± 4.33	15.79	5	0.90 ± 3.22	10.53
<i>Eualus</i> sp2.	0	0.00	0.00	1	0.18 ± 0.79	5.26
<i>Processa</i> spp.	11	1.50 ± 3.69	26.32	5	0.83 ± 3.18	10.53
<i>Plesionika</i> spp.	4	0.54 ± 1.39	15.79	5	1.09 ± 3.65	10.53
Pontoninae	0	0.00	0.00	1	0.13 ± 0.56	5.26
Pandalidae	0	0.00	0.00	4	0.56 ± 1.42	15.79
Caridea sp1	2	0.44 ± 1.41	10.53	0	0.00	0.00
Caridea sp2	3	0.74 ± 2.65	10.53	0	0.00	0.00
Caridea sp3	2	0.60 ± 2.61	5.26	0	0.00	0.00
Caridea	6	0.87 ± 1.38	31.58	0	0.00	0.00
Scyllaridae	0	0.00	0.00	1	0.12 ± 0.53	5.26
<i>Scyllarus</i> spp.	5	0.62 ± 1.72	15.79	1	0.13 ± 0.58	5.26
Callianassidae	0	0.00	0.00	2	0.39 ± 1.26	10.53
<i>Upogebia</i> spp.	1	0.21 ± 0.91	5.26	1	0.10 ± 0.45	5.26
<i>Galathea</i> spp.	2	0.44 ± 1.94	5.26	0	0.00	0.00
<i>Calcinus tubularis</i>	6	0.96 ± 3.36	10.53	6	1.07 ± 3.43	10.53
<i>Dardanus</i> spp.	21	2.52 ± 3.68	52.63	24	3.13 ± 3.80	57.89
<i>Dardanus arrosor</i>	0	0.00	0.00	1	0.17 ± 0.75	5.26
<i>Anapagurus</i> spp.	1	0.21 ± 0.91	5.26	0	0.00	0.00
<i>Maja</i> sp1	1	0.21 ± 0.91	5.26	0	0.00	0.00
<i>Maja</i> sp2	1	0.21 ± 0.91	5.26	0	0.00	0.00
<i>Achaeus / Inachus</i> spp.	3	0.49 ± 2.13	5.26	0	0.00	0.00
<i>Ebalia</i> spp.	4	0.72 ± 1.89	15.79	6	0.91 ± 1.86	21.05
<i>Calappa granulata</i>	4	0.67 ± 1.50	21.05	2	0.36 ± 1.59	5.26
<i>Pirimela denticulata</i>	2	0.26 ± 0.77	10.53	0	0.00	0.00
Polybiinae	3	0.62 ± 1.59	15.79	0	0.00	0.00
Parthenopidae	8	1.30 ± 5.69	5.26	10	1.62 ± 4.11	26.32
<i>Eriphia verrucosa</i>	1	0.30 ± 1.31	5.26	0	0.00	0.00
<i>Xantho</i> spp.	6	0.92 ± 2.89	15.79	11	1.06 ± 2.51	21.05
<i>Xantho incisus</i>	0	0.00	0.00	1	0.18 ± 0.79	5.26
<i>Pilumnus</i> spp.	1	0.21 ± 0.91	5.26	1	0.18 ± 0.79	5.26
<i>Goneplax rhomboides</i>	1	0.12 ± 0.53	5.26	0	0.00	0.00
Grapsoidea	2	0.34 ± 1.07	0.00	1	0.18 ± 0.79	0.00
Brachyura sp1	1	0.22 ± 0.97	10.53	0	0.00	5.26
Brachyura sp2	1	0.22 ± 0.97	5.26	0	0.00	0.00
Brachyura	1	0.15 ± 0.66	5.26	0	0.00	0.00
Non-identified	5	0.67 ± 1.57	5.26	2	0.27 ± 0.81	0.00
Total	296	44.01 ± 47.20		165	23.44 ± 24.66	

Table 4. – Total number (N) of decapod larvae caught with MOCNESS sampler.

Taxon	N	Average density (ind./1000 m ³)	F (%)
Suborder Dendrobranchiata			
<i>Aristeus antennatus</i>	2	0.79 ± 1.36	33.33
<i>Sergestidae</i>	14	5.08 ± 1.99	100.00
<i>Solenocera membranacea</i>	35	21.66 ± 33.83	100.00
Suborder Pleocyemata			
<i>Acanthephyra</i> spp.	1	0.54 ± 0.93	33.33
<i>Alpheus glaber</i>	40	25.67 ± 22.25	100.00
<i>Athanas nitescens</i>	1	0.88 ± 1.52	33.33
<i>Eualus</i> spp.	4	2.39 ± 2.41	66.67
<i>Processa novveli</i>	1	0.88 ± 1.52	33.33
<i>Processa</i> spp.	12	5.97 ± 10.34	33.33
<i>Plesionika</i> spp.	13	6.77 ± 11.72	33.33
Pandalidae	3	1.07 ± 1.86	33.33
<i>Scyllarus</i> spp.	5	1.68 ± 2.91	33.33
Scyllaridae	2	0.00	0.00
<i>Polycheles typhlops</i>	2	1.22 ± 2.11	33.33
<i>Galathea</i> spp.	3	0.00	0.00
<i>Calcinus tubularis</i>	2	0.79 ± 1.36	33.33
<i>Dardanus</i> spp.	2	0.53 ± 0.93	33.33
<i>Dardanus arrosor</i>	1	0.00	0.00
<i>Nematopagurus longicornis</i>	2	0.00	0.00
<i>Pagurus</i> spp.	1	0.50 ± 0.86	33.33
<i>Inachus</i> spp.	1	0.88 ± 1.52	33.33
<i>Ebalia</i> spp.	3	1.53 ± 2.72	33.33
<i>Ilia nucleus</i>	4	1.13 ± 1.18	66.67
<i>Polybiinae</i>	2	1.53 ± 2.72	33.33
Parthenopidae	6	2.45 ± 2.36	66.67
Geryonidae	1	0.00	0.00
<i>Xantho</i> spp.	4	0.88 ± 1.52	33.33
<i>Goneplax rhomboides</i>	4	3.06 ± 3.99	66.67
Brachyura	1	0.79 ± 1.36	33.33
Non-identified	2	0.00	0.00
Total	174		

species or groups that were responsible for the differences between canyon zones.

RESULTS

Identification and taxonomic assignment of decapod larvae

The total number of larvae and density by taxon are shown in Tables 3 (bongo samples) and 4 (MOCNESS samples). A total of 635 decapod larvae belonging to 66 taxa were sorted, and 426 of them were identified at least to the genus level by morphological characters. Molecular analyses were used to discriminate between PZI larvae of *A. antennatus* and *G. elegans*.

The pool sample containing the 35 protozoa individuals showed one high-abundance haplotype and 186 additional haplotypes, all belonging to *A. antennatus*. A search within the unfiltered OTU table, aimed at detecting possible low-abundance sequences of other species that might have been removed during the filtering process, revealed only sequences belonging to *A. antennatus*. The best match in the reference databases showed a 100% overlap identity with the pool sample sequences with a query cover of 163/172 base pairs.

Decapod larval communities

Both nets B300 and B500 caught mainly shrimp larvae: B300 caught more Dendrobranchiata (43% of the total catch) and B500 more Caridea (42% of the to-

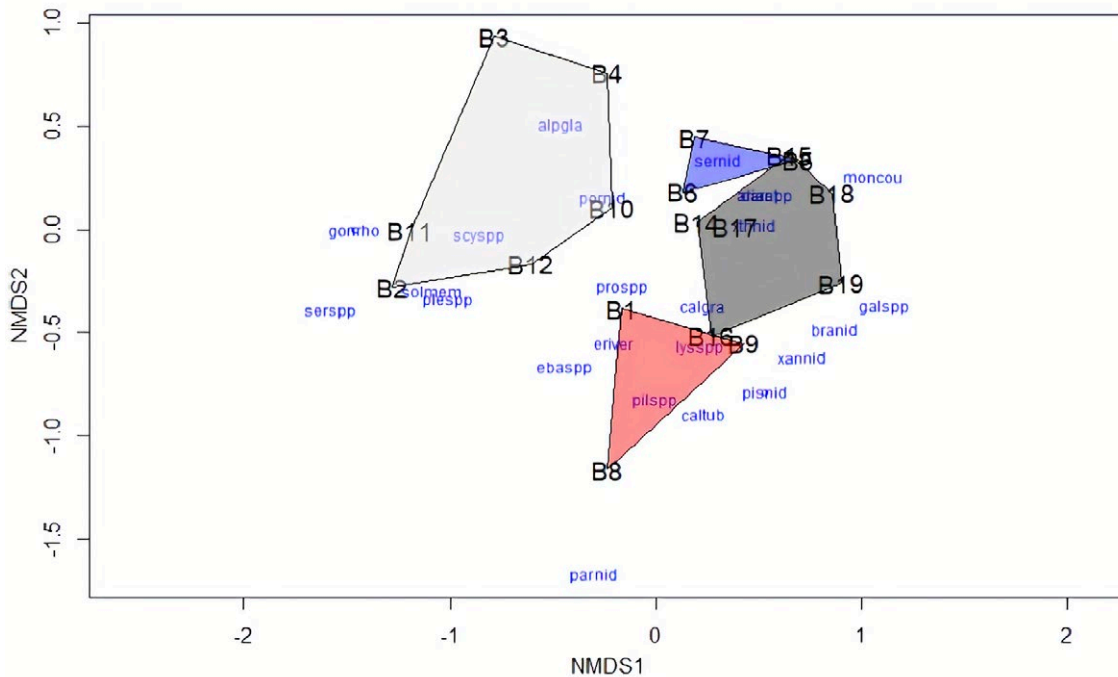


Fig. 2. – Non-metric multidimensional scaling analysis (stress=0.1734). Polygon colours indicate canyon zones: upstream wall (white), canyon axis (blue), downstream wall (grey), canyon head (red). Station B13, with no decapod larvae, is not shown. Ariant, *Aristeus antennatus*; sermid, Sergestidae; serspp, *Sergia* spp.; seratl, *Sergestes atlanticus*; solmem, *Solenocera membranacea*; siccar, *Sicyonia carinata*; alpgla, *Alpheus glaber*; easpp, *Eualus* spp.; lysspp, *Lyssmata* spp.; prospp, *Processa* spp.; plespp, *Plesionika* spp.; passpp, *Pasiphaea* spp.; carnid, unidentified Caridea; darspp, *Dardanus* spp.; caltub, *Calcinus tubularis*; anaspp, *Anapagurus* spp.; galspp, *Galathea* spp.; scyspp, *Scyllarus* spp.; upospp, *Upogebia* spp.; pornid, Portunidae; pisinid, Pisidae; inanid, Inachidae; xthnid, Xanthoidea; xannid, Xanthidae; xanspp, *Xantho* spp.; parnid, unidentified Parthenopidae; gonrho, *Goneplax rhomboides*; ebaspp, *Ebalia* spp.; pilspp, *Pilumnus* spp.; calgra, *Calappa granulata*; eriver, *Eriphia verrucosa*; moncou, *Monodaeus couchii*; branid, unidentified Brachyura. Data from B300.

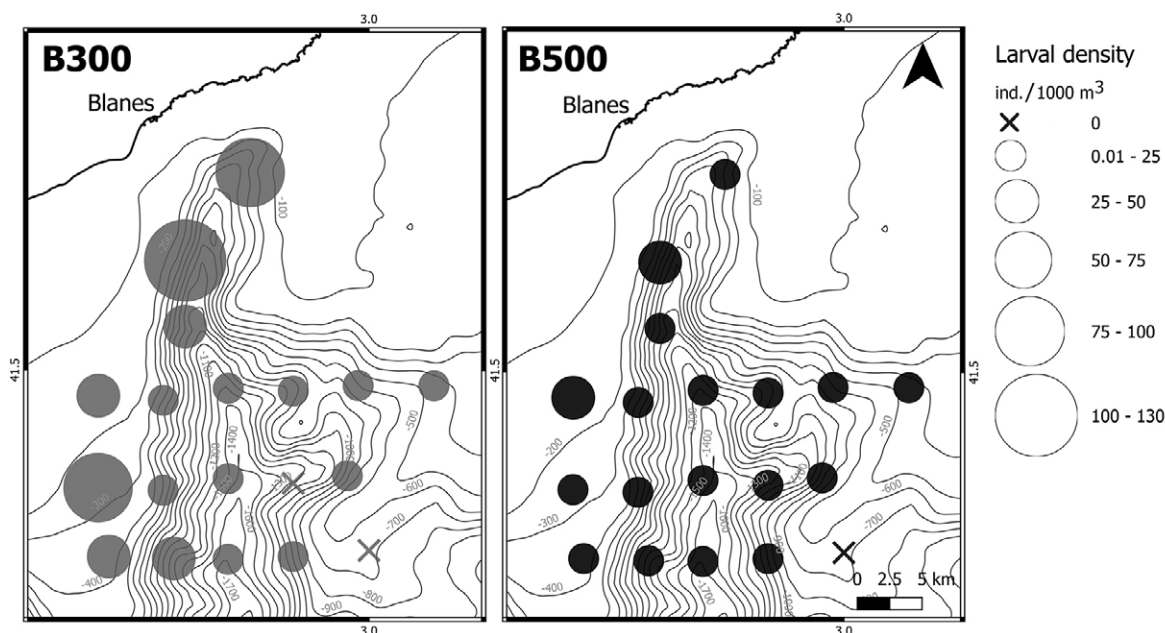


Fig. 3. – Density of early (B300, stages I to III) and late (B500, stages VI to decapodid) larval stages of all decapod larvae in individuals (ind.) per 1000 m³.

tal catch). Due to the low number of individuals caught in B500 and MOCNESS samples, statistical analysis could only be performed with B300 data.

The NMDS representation for B300 data (Fig. 2, stress=0.1734) shows a grouping of the communities separating two spatial regions: one composed of the upstream wall and one composed of the rest of the canyon zones. After applying a Bonferroni correction to a pairwise analysis by canyon zone, the distance between the communities was only significant between the upstream and downstream walls of the canyon ($p=0.018$). The SIMPER analysis showed that the downstream wall community is characterized by the presence of *A. antennatus* and larvae of the family Sergestidae, which together explain 43.2% of the dissimilarity from the community of the upstream wall. The relationship between the NMDS ordination and the environmental variables (sea surface temperature and surface chlorophyll *a* concentration) was not significant.

Average larval stages of decapod larvae were significantly different in B300 (3.75) and B500 (6.26) ($p=0.003$). Early larval stages (I to IV) were extracted from B300 and late stages (VI to IX) from B500, and are represented separately for comparison in Figure 3. Both early and late stages show a higher aggregation at the canyon head and downstream wall, although early stages show higher density values.

Decapod larvae density and distribution

Total decapod larval density values ranged from 5.79 (station B4, located at the upstream canyon wall) to 188.99 ind./1000 m³ (station B8, located at the canyon head). The decapod larva distribution in the canyon is shown in Figure 4. The highest average density (7.93 ind./1000 m³) corresponded to the first protozoal stage of the deep-sea blue and red shrimp *Aristeus antennatus*. The second most abundant larvae were protozoas

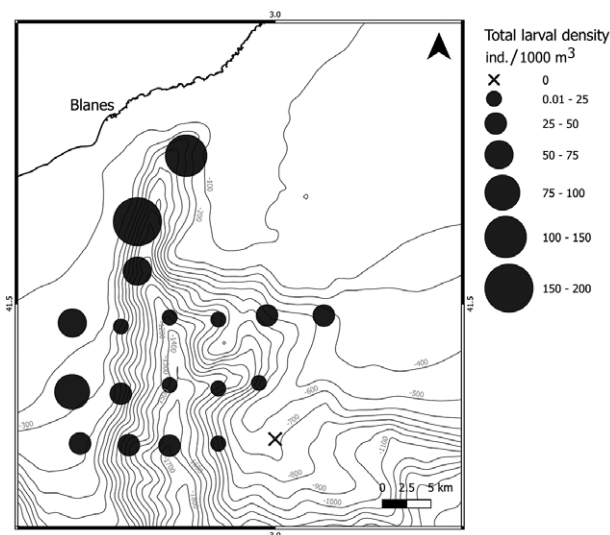


Fig. 4. – Total decapod larvae density in individuals (ind.) per 1000 m³ for B300.

of the family Sergestidae (7.24 ind./1000 m³), which includes the very common small mesopelagic shrimp *Eusergestes arcticus*. The larvae of the mud shrimp *Alpheus glaber* were the third most abundant species caught (average density 6.78 ind./1000 m³), followed at a considerable distance by the larvae of the hermit crab taxa, *Dardanus* spp. These three most abundant taxa were also the most frequent, showing frequencies higher than 60%. Their spatial distribution, presented in Figure 5, shows that both *A. antennatus* and the Sergestidae are more abundant at the canyon head and the downstream wall. On the other hand, *Alpheus glaber* larvae are found more abundantly at the canyon head and upstream wall.

Total decapod larval density and Shannon diversity index were significantly higher at the canyon

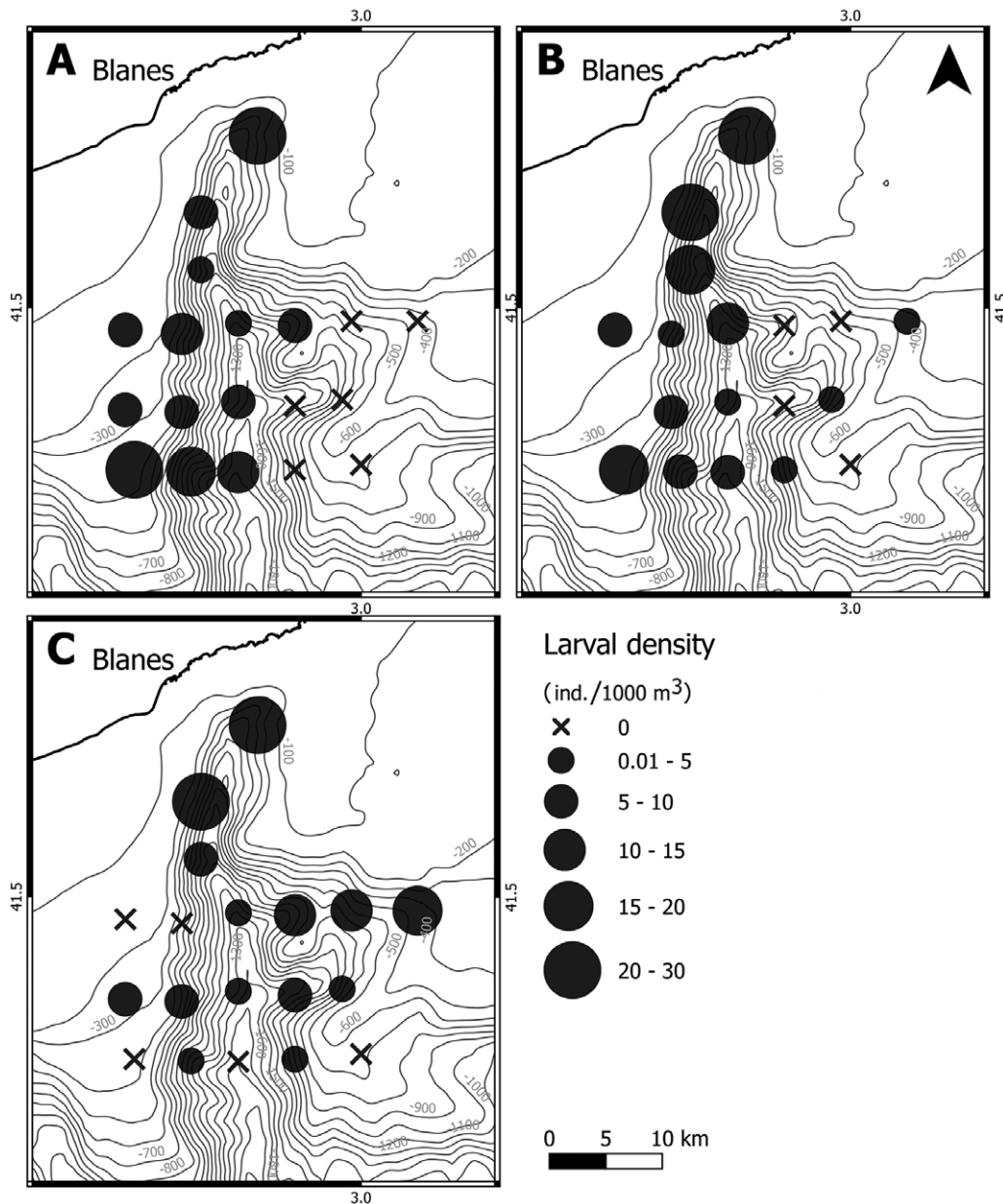


Fig. 5. – Larval density of most frequent species (individuals/1000 m³) for B300. A, *Aristeus antennatus*.; B, Sergestidae; C, *Alpheus glaber*.

head than the upstream wall (Fig. 6A-B; $p=0.003$ and $p=0.037$, respectively). Likewise, species richness was significantly higher at the canyon head than in all the other canyon zones (Fig. 6C; $p=0.008$). Species evenness showed no significant differences across canyon zones (Fig. 6D). Excluding station B3, which featured only one species of decapod larvae, species evenness was between 0.76 and 0.97. No decapod larvae were found at station B13. During this particular bongo tow, a large colony of medusae was observed at the surface.

As for the stratified MOCNESS samples, the larvae were aggregated in the first 100 m of the water column (Fig. 7). The families Alpheidae and Solenoceridae were the most abundant throughout the MOCNESS samples. One *A. antennatus* PZ I larva was caught at station MN03 between 50 and 100 m depth. Two rare *Polycheles typhlops* (Polychelidae)

zoa II larvae were found between 300 and 500 m depth at station MN03.

Atmospheric and surface water characteristics

An anticyclonic gyre governed local hydrodynamics over the Blanes canyon on the days of the sample collection, as reported by the reanalysis product (Fig. 8). According to these data, the anticyclonic gyre was weak (~ 0.10 m s⁻¹), approximately 30 km wide, and covered the upper 50 m depth. According to the OOCs database and the oceanographic buoy, the average daily current was stronger than that of the reanalysis, with values between 0.35 and 0.22 m s⁻¹ from the surface to 50 m depth. The current speed fell from 0.12 m s⁻¹ to 0.06 m s⁻¹ from 60 to 100 m depth. The NE direction of the current was consistent with that of the reanalysis (60°-80°) up to 60 m depth, and then de-

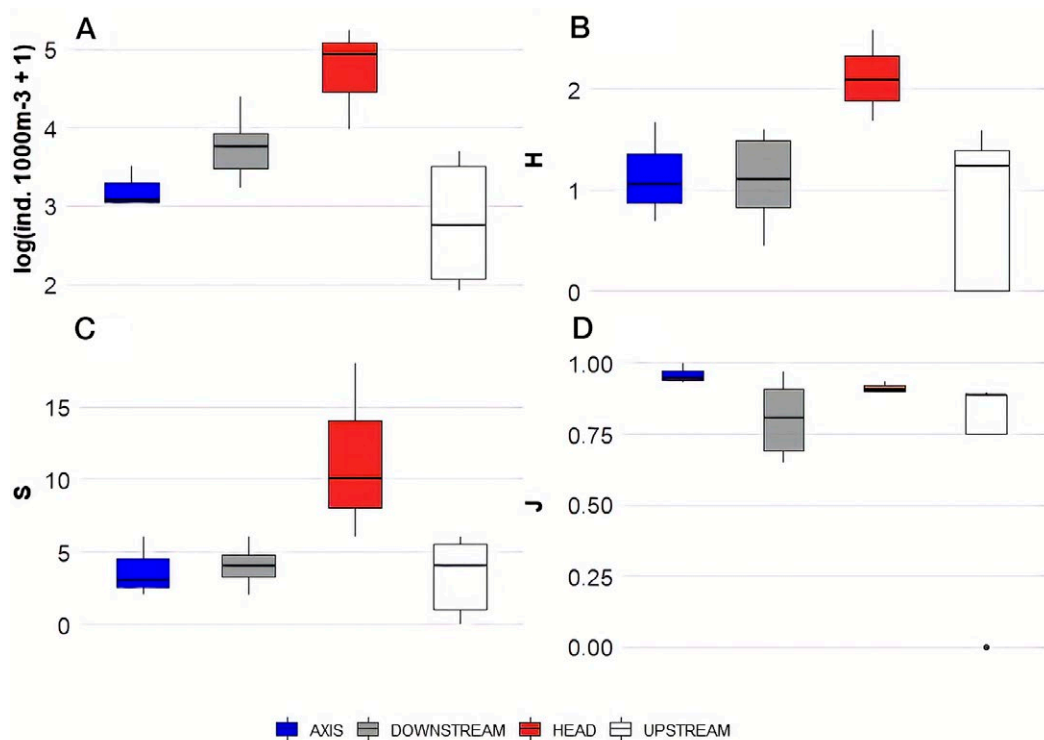


Fig. 6. – Box and whisker diagrams showing median, third quartiles and minimum and maximum values by zone for A, decapod larval density ($\log(\text{ind.}/1000\text{ m}^3)+1$); B, Shannon diversity index (H); C, species richness (S); D, Pielou evenness index (J). Data from B300.

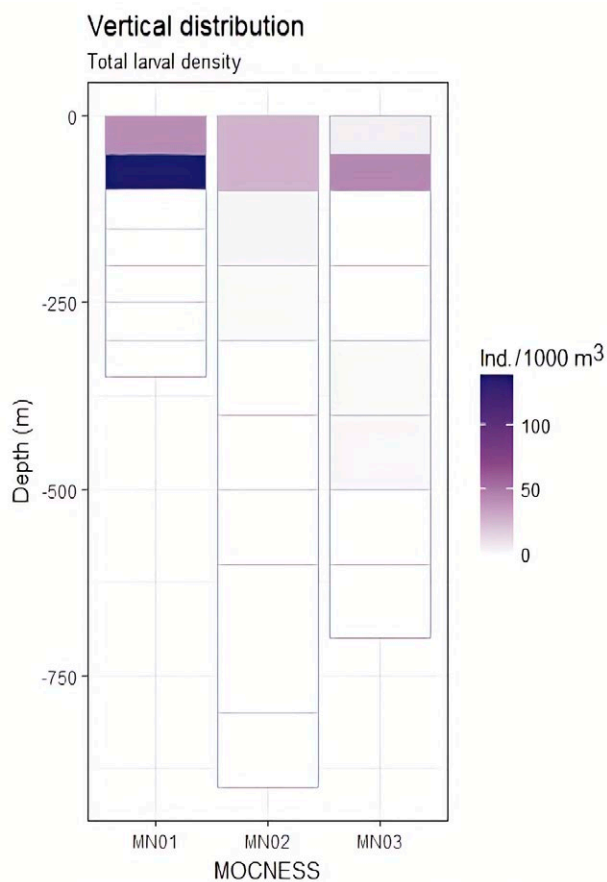


Fig. 7. – Abundance of decapod larvae at MOCNESS stations MN01, MN02 and MN03 in relation to sampling depth strata.

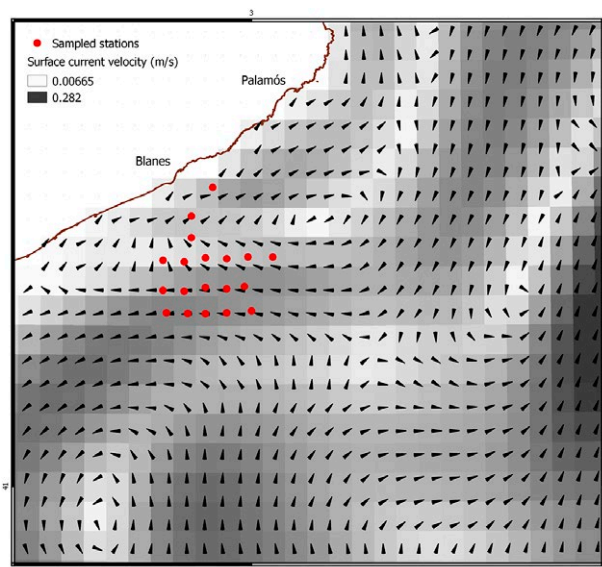


Fig. 8. – Average surface current velocity from reanalysis (<http://marine.copernicus.eu/>) during the month of September 2011. Red dots represent the sampled stations. Black arrows represent the direction of the current.

viated SE (130° - 170°) between 70 and 100 m depth. The database reported an average air temperature of 22.6°C , an atmospheric pressure of 1023 hPa and average southward winds of 2.8 m s^{-1} .

DISCUSSION

This study offers initial information on the larval distribution of *A. antennatus* in the northwestern Medi-

terranean Sea. The decapod crustacean larval communities described differ from those of previous studies in the northwestern Mediterranean Sea (Fusté 1987, Torres et al. 2014a), mainly due to the predominance of larvae of the deep-sea blue and red shrimp *Aristeus antennatus* in our study. Our results support the hypothesis that the Blanes submarine canyon is an important spawning area for *A. antennatus*, because its first protozoal stage, which occurs shortly after spawning, was found to be the dominant taxon in the decapod larval community at the end of the reproductive period of the species, i.e. late September. In addition, the occurrence of one PZ I larva of the species below the upper 70 m where they have been reported in earlier studies (e.g. Heldt 1955, Carbonell et al. 2010, Carreton et al. 2019) shows the importance of performing more stratified samplings to further evaluate the vertical distribution pattern of these larvae. These findings also support the model proposed by Carbonell et al. (2010), which considers that the first protozoal stage performs an ontogenetic migration through the water column to surface layers, where the subsequent larval stages will develop.

The larvae of the family Sergestidae have been cited as a predominant taxon in the plankton of offshore waters of the northwestern Mediterranean throughout the year (Torres et al. 2014a, Simão et al. 2014). Some genera of this family, particularly *Eusergestes arcticus*, are accidentally caught in the nets of bottom trawlers in the area (Gorelli et al. 2016). The presence of protozoal stages of these species in the submarine canyon indicates proximity to the spawning grounds. The mud shrimp *Alpheus glaber* is very common in Mediterranean waters, and ovigerous females of the species can be found in March and August (Zariquiey-Álvarez 1968). Its larvae have been previously found in the northwestern Mediterranean (Fusté 1987, Torres et al. 2014a), although in lower numbers than those obtained in the present study. The two *Polycheles typhlops* larvae from this study were identified through molecular methods, described, and included in a phylogenetic analysis (Torres et al. 2014b).

The highest diversity and species richness found in the submarine canyon head supports the idea that submarine canyons are key structures for many species, which aggregate in these areas for spawning (Sardà et al. 2009, Fernandez-Arcaya et al. 2013). The upstream and downstream walls of the canyon host significantly different communities of decapod larvae. Aside from the influence of the local circulation pattern, this distribution could be explained by a patchy distribution of zooplankton but, especially in the case of the early zoeal stages, it also provides information on the habitat

preferences of the species during the spawning period. A paired study of decapod adult and larva distribution is desirable to account for dispersal capacity and habitat preferences of the different life stages of the species.

Modelling exercises of particle dispersal carried out in previous studies (Ahumada-Sempoal et al. 2015) have suggested that particles released upstream (on the eastern wall of the canyon) show greater retention rates over the canyon head than over its surroundings. In these theoretical experiments, retention of around 40% of the particles takes place at depths shallower than 100 m when the particles are released above the shelf break at 150 m depth. In our study, considering the water circulation described for Blanes canyon (Flexas et al. 2008), the general abundance values were higher at the stations that follow the main path of the Northern Current: B12, B11, B8, B19, B16 and B14.

The distribution pattern of the larvae was similar for early and late larval stages, but densities were higher overall for the former, probably due to their high mortality. A similar distribution pattern throughout larval stages indicates a good larval retention in the area. In addition, the circulation pattern in the canyon probably favoured the retention of larvae from adult individuals inhabiting the area as opposed to an import of larvae from nearby areas. The vertical distribution of summer chlorophyll *a* in the northwestern Mediterranean, with a deep chlorophyll maximum located above 100 m depth according to in situ historical data from the oceanographic buoy of the OOCSS located at Blanes canyon head (Bahamon et al. 2011). A study including more stratified (MOCNESS) samples and thorough in situ oceanographic data needs to be conducted to further explore the influence of water mass circulation in decapod larva distribution.

We expected relatively high densities of decapod larvae in our area due to summer stratification conditions and the role of the canyon as a retention zone (Ahumada-Sempoal et al. 2015), but the overall larval density values obtained for our study were much lower than those of previous studies in nearby areas (Table 5). These values may be related to the sampling period being at the end of September, when most decapod species have ended their reproduction period and larvae have already settled and/or recruited to the adult habitats. The relatively low total density of crustacean larvae may also be related to the presence of a transient anticyclonic gyre, as reported by the oceanographic reanalysis data. According to Ahumada-Sempoal et al. (2015), this gyre affects the area during the summer months and is formed over the slope as a consequence of a counter-current flowing northeastwards, parallel to

Table 5. – Comparison of up-to-date studies on decapod larval communities in the western Mediterranean Sea.

Publication	Study area	Time of year	Bottom depth (m)	Sampling method	Average decapod larval density (ind./1000 m ³)
Fusté 1987	Catalan coast (shelf)	September	50 200	Bongo net (integrated)	10000
Torres et al. 2014a	Balearic Islands	July	250 900	MOCNESS (stratified)	144.5 (Northern area) 85.3 (Southern area)
This study	Catalan margin (Blanes submarine canyon)	September	150-1700	Bongo net (integrated)	23.38

the coast (NE direction), opposed to the southward offshore current generated by northern winds. Meanders and anticyclonic eddies are recurrent in Blanes canyon, producing high fluctuations in the three-dimensional circulation patterns within the canyon (Flexas et al. 2008). Transient anticyclonic gyres of this sort may form over the canyon head, altering the general distribution pattern of particles and living organisms such as eggs and larvae (Ahumada-Sempoal et al. 2015).

Larval ecology remains one of the main knowledge gaps in marine science, and additional studies are still needed before we can move on to further analysis of the communities. In coastal species, biophysical models have helped understand the influence of oceanic currents and tides in the transport and settlement of decapod larvae (e.g. Pires et al. 2013, Criales et al. 2015). In the case of deep-sea species larvae, once evidence of larval presence has been reported, a reasonable next step is to explore the combined potential of stratified field samplings, oceanographic data and biophysical modelling to explain their distribution.

CONCLUSIONS

The decapod larval community of Blanes canyon at the end of September is dominated by three taxa: the deep-sea blue and red shrimp *Aristeus antennatus*, the family Sergestidae and the mud shrimp *Alpheus glaber*. Decapod larval communities are richer and more diverse at the canyon head than on the upstream and downstream walls and in the canyon axis.

ACKNOWLEDGEMENTS

This research was carried out within project OAMMS (CTM2008-03983), financed by the Spanish *Ministerio de Economía y Competitividad*. Molecular analyses were done by AllGenetics (A Coruña, Spain).

Data availability

The datasets generated and/or analysed during the current study are available from the corresponding author on reasonable request.

Conflict of interest

During the writing of this manuscript, MC was supported by a grant from the Spanish Ministerio de Educación (FPU2015). All authors declare that we have no conflict of interest with funding sources or with the submission of this manuscript.

REFERENCES

Abelló P. 1989. Reproduction and moulting in *Liocarcinus depurator* (Linnaeus, 1758) (Brachyura: Portunidae) in the Northwestern Mediterranean Sea. *Sci. Mar.* 53: 127-134.
 Abelló P., Guerao G. 1999. Temporal variability in the vertical and mesoscale spatial distribution of crab megalopae (Crustacea: Decapoda) in the Northwestern Mediterranean. *Estuar. Coast. Shelf Sci.* 49: 129-139.
<https://doi.org/10.1006/ecss.1999.0488>
 Ahumada-Sempoal M.A., Flexas M.M., Bernardello R., et al. 2013.

Northern Current variability and its impact on the Blanes Canyon circulation: A numerical study. *Prog. Oceanogr.* 118: 61-70.
<https://doi.org/10.1016/j.pocean.2013.07.030>
 Ahumada-Sempoal M.A., Flexas M.M., Bernardello R., et al. 2015. Shelf-slope exchanges and particle dispersion in Blanes submarine canyon (NW Mediterranean Sea): A numerical study. *Cont. Shelf. Res.* 109: 35-45.
<https://doi.org/10.1016/j.csr.2015.09.012>
 Bahamon N., Aguzzi J., Bernardello R., et al. 2011. The new pelagic Operational Observatory of the Catalan Sea (OOCs) for the multisensor coordinated measurement of atmospheric and oceanographic conditions. *Sensors* 11: 11251-11272.
<https://doi.org/10.3390/s111211251>
 Boletín Oficial del Estado (BOE). 2018. Orden APM/532/2018, de 25 de mayo, por la que se regula la pesca de gamba rosada (*Aristeus antennatus*) con arte de arrastre de fondo en determinadas zonas marítimas próximas a Palamós. 128. Sábado 26 de mayo de 2018 (Sección III): 55045-55051.
 Canals M., Company J.B., Martín D., et al. 2013. Integrated study of Mediterranean deep canyons: Novel results and future challenges. *Prog. Oceanogr.* 118: 1-27.
<https://doi.org/10.1016/j.pocean.2013.09.004>
 Campos P.F., Gilibert T.M. 2012. DNA extraction from formalin-fixed material. *Methods Mol. Biol.* 840: 81-85.
https://doi.org/10.1007/978-1-61779-516-9_11
 Carbonell A., dos Santos A., Alemany F., et al. 2010. Larvae of the red shrimp *Aristeus antennatus* (Decapoda: Dendrobranchiata: Aristeidae) in the Balearic Sea: new occurrences fifty years later. *Mar. Biodivers. Rec.* 3: E103.
<https://doi.org/10.1017/S1755267210000758>
 Carreton M., Company J.B., Planella L., et al. 2019. Morphological identification and molecular confirmation of the deep-sea blue and red shrimp *Aristeus antennatus* larvae. *PeerJ* 7: e6063.
<https://doi.org/10.7717/peerj.6063>
 Company J.B., Sardà F. 2000. Growth parameters of deep-water decapod crustaceans in the Northwestern Mediterranean Sea: a comparative approach. *Mar. Biol.* 136: 79-90.
<https://doi.org/10.1007/s002270050011>
 Company J.B., Sardà F., Puig P., et al. 2003. Duration and timing of reproduction in decapod crustaceans of the NW Mediterranean continental margin: Is there a general pattern? *Mar. Ecol. Prog. Ser.* 261: 201-216.
<https://doi.org/10.3354/meps261201>
 Caporaso J.G., Kuczynski J., Stombaugh J., et al. 2010. QIIME allows analysis of high-throughput community sequencing data. *Nat. Methods* 7: 335-336.
<https://doi.org/10.1038/nmeth.f.303>
 Criales M.M., Zink I.C., Haus B.K., et al. 2013. Effect of turbulence on the behavior of pink shrimp postlarvae and implications for selective tidal stream transport behavior. *Mar. Ecol. Prog. Ser.* 477: 161-176.
<https://doi.org/10.3354/meps10141>
 Criales M.M., Cherubin L.M., Browder J.A. 2015. Modeling Larval Transport and Settlement of Pink Shrimp in South Florida: Dynamics of Behavior and Tides. *Mar. Coast. Fish.* 7: 148-176.
<https://doi.org/10.1080/19425120.2014.1001541>
 De Leo F.C., Smith C.R., Rowden A.A., et al. 2010. Submarine canyons: hotspots of benthic biomass and productivity in the deep sea. *Proc. Royal Soc. B.: Biol. Sci.* 277: 2783-2792.
<https://doi.org/10.1098/rspb.2010.0462>
 dos Santos A., González-Gordillo J.I. 2004. Illustrated keys for the identification of the Pleocyemata (Crustacea: Decapoda) zoeal stages, from the coastal region of south-western Europe. *J. Mar. Biol. Assoc. UK* 84: 205-227.
<https://doi.org/10.1017/S0025315404009075h>
 dos Santos A., Lindley J.A. 2001. Crustacea Decapoda: Larvae II. Dendrobranchiata (Aristeidae, Benthescymidae, Penaeidae, Solenoceridae, Sicyonidae, Sergestidae, and Luciferidae). ICES Identification Leaflets for Plankton.
 Fernandez-Arcaya U., Rotllant G., Ramirez-Llodra E., et al. 2013. Reproductive biology and recruitment of the deep-sea fish community from the NW Mediterranean continental margin. *Prog. Oceanogr.* 118: 222-234.
<https://doi.org/10.1016/j.pocean.2013.07.019>
 Flexas M.M., Boyer D.L., Espino M., et al. 2008. Circulation over a submarine canyon in the NW Mediterranean. *J. Geophys. Res.: Oceans* 113: 1-18.
<https://doi.org/10.1029/2006JC003998>
 Fusté X. 1987. Distribución de larvas de Crustáceos Decápodos de la costa de Cataluña. *Inv. Pesq.* 51: 277-284.

- Gili J.M., Pagès F., Bouillon J., et al. 2000. A multidisciplinary approach to the understanding of hydromedusan populations inhabiting Mediterranean submarine canyons. *Deep. Sea Res. Part 1 Oceanogr. Res. Pap.* 47: 1513-1533.
[https://doi.org/10.1016/S0967-0637\(99\)00119-3](https://doi.org/10.1016/S0967-0637(99)00119-3)
- González-Gordillo J., Dos Santos A., Rodríguez A. 2001. Checklist and annotated bibliography of decapod crustacean larvae from the Southwestern European coast (Gibraltar Strait area). *Sci. Mar.* 65: 275-305.
<https://doi.org/10.3989/scimar.2001.65n4275>
- Gorelli G., Blanco M., Sardà F., et al. 2016. Spatio-temporal variability of discards in the fishery of the deep-sea red shrimp *Aristeus antennatus* in the northwestern Mediterranean Sea: implications for management. *Sci. Mar.* 80: 79-88.
<https://doi.org/10.3989/scimar.04237.24A>
- Granata T.C., Vidondo B., Duarte C.M., et al. 1999. Hydrodynamics and particle transport associated with a submarine canyon off Blanes (Spain), NW Mediterranean Sea. *Cont. Shelf Res.* 19: 1249-1263.
[https://doi.org/10.1016/S0278-4343\(98\)00118-6](https://doi.org/10.1016/S0278-4343(98)00118-6)
- Gurney R. 1924. Decapod larvae. Part IX. British Antarctic (Terra Nova) Expedition. *Nat. Hist. Rep. Terra Nova Exped.* 8: 38-200.
- Heldt J.H. 1955. Contribution à l'étude de la biologie des crevettes péneïdes *Aristaeomorpha foliacea* (Risso) et *Aristeus antennatus* (Risso) (Formes larvaires). *Bull. Soc. Sci. Nat. Tunisie VIII 1-2*: 1-29.
- Leinonen R., Sugawara H., Shumway M. 2010. International Nucleotide Sequence Database Collaboration. The sequence read archive. *Nucleic Acids Res.* 39 (Database issue): D19-D21.
<https://doi.org/10.1093/nar/gkq1019>
- Magoc T., Salzberg S.L. 2011. FLASH: fast length adjustment of short reads to improve genome assemblies. *Bioinformatics* 27: 2957-2963.
<https://doi.org/10.1093/bioinformatics/btr507>
- Martin M. 2011. Cutadapt removes adapter sequences from high-throughput sequencing reads. *EMBnet J.* 17: 10-12.
<https://doi.org/10.14806/ej.17.1.200>
- Maynou F., Conan G.Y., Cartes J.E., et al. 1996. Spatial structure and seasonality of decapod crustacean populations on the northwestern Mediterranean slope. *Limnol. Oceanogr.* 41: 113-125.
<https://doi.org/10.4319/lo.1996.41.1.0113>
- Oksanen J., Blanchet F.J., Friendly M., et al. 2017. vegan: Community Ecology Package. R package version 2.4-4.
- Pires R.F.T., Pan M., Santos A.M.P., et al. 2013. Modelling the variation in larval dispersal of estuarine and coastal ghost shrimp: *Upogebia* congeners in the Gulf of Cadiz. *Mar. Ecol. Prog. Ser.* 492: 153-168.
<https://doi.org/10.3354/meps10488>
- QGIS Development Team. 2019. QGIS Geographic Information System. Open Source Geospatial Foundation.
<http://qgis.osgeo.org>
- R Development Core Team. 2018. R: A language and environment for statistical computing. R Foundation for Statistical Computing, Vienna, Austria.
<http://www.R-project.org>
- Rubio A., Arnau P.A., Espino M., et al. 2005. A field study of the behaviour of an anticyclonic eddy on the Catalan continental shelf (NW Mediterranean). *Progr. Oceanogr.* 66: 142-156.
<https://doi.org/10.1016/j.pocean.2004.07.012>
- Sardà F., Company J.B., Bahamón N., et al. 2009. Relationship between environment and the occurrence of *Aristeus antennatus* (Risso, 1816) in the Blanes submarine canyon (NW Mediterranean). *Progr. Oceanogr.* 82: 227-238
<https://doi.org/10.1016/j.pocean.2009.07.001>
- Simão D.S., Torres A.P., Olivar M.P., et al. 2014. Vertical and temporal distribution of pelagic decapod crustaceans over the shelf-break and middle slope in two contrasting zones around Mallorca (western Mediterranean Sea). *J. Mar. Syst.* 138: 139-149.
<https://doi.org/10.1016/j.jmarsys.2013.10.008>
- Steinke D., Prosser S.W.J., Hebert P.D.N. 2016. DNA barcoding of marine metazoans; In: Bourlat S (ed), *Marine Genomics. Methods in Molecular Biology* 1452: 155-168. Humana Press, New York, NY.
https://doi.org/10.1007/978-1-4939-3774-5_10
- Torres A.P., dos Santos A., Alemany F., et al. 2013. Larval stages of crustacean species of interest for conservation and fishing exploitation in the western Mediterranean. *Sci. Mar.* 77: 149-160.
<https://doi.org/10.3989/scimar.03749.26D>
- Torres A.P., dos Santos A., Balbín R., et al. 2014a. Decapod crustacean larval communities in the Balearic Sea (western Mediterranean): Seasonal composition, horizontal and vertical distribution patterns. *J. Mar. Syst.* 138: 112-126.
<https://doi.org/10.1016/j.jmarsys.2013.11.017>
- Torres A.P., Palero F., Dos Santos A., et al. 2014b. Larval stages of the deep-sea lobster *Polycheles typhlops* (Decapoda, Polychelida) identified by DNA analysis: Morphology, systematic, distribution and ecology. *Helgol. Mar. Res.* 68: 379-397.
<https://doi.org/10.1007/s10152-014-0397-0>
- Wiebe P.H., Burt K.H., Boyd S.H., et al. 1976. A multiple opening/closing net and environmental sensing system for sampling zooplankton. *J. Mar. Res.* 34: 313-326.
- Zariquiey Álvarez, R. 1968. Crustáceos decápodos ibéricos. *Inv. Pesq.* 32: 1-510.